Nano-Fe₃O₄ Encapsulated-Silica Particles Bearing Sulfonic Acid Groups as a Magnetically Separable Catalyst for Highly Efficient Knoevenagel Condensation and Michael Addition Reactions of Aromatic Aldehydes with 1,3-Cyclic Diketones

Firouzeh NEMATI[1,*], Majid M. HERAVI[2], Raheleh SAEEDI RAD[1]

[1]*Department of Chemistry, Semnan University, Semnan, Iran*

[2]*Department of Chemistry, School of Science, Azzahra University, Vanak, Tehran, Iran*

Abstract: Sulfonic acid-functionalized silica-coated nano-Fe₃O₄ particles (Fe₃O₄@SiO₂-SO₃H) have been prepared as a novel heterogeneous acid using a facile process. The material was subsequently identified as an efficient catalyst for the synthesis of a variety of tetraketone derivatives via the Knoevenagel condensation and Michael addition reactions of aromatic aldehydes to dimedone, 1,3-indanedione, and 1,3-dimethyl barbituric acid. The catalyst could be readily recovered using a simple external magnet and reused several times without any significant loss in activity. The current catalytic process is both sustainable and economical because it operates under aqueous conditions, the catalyst can be recovered and reused, and the reactions themselves require only a short time and provide the products in high yield.

Key words: magnetic nanoparticle; silica; Knoevenagel condensation; Michael addition; cyclic diketone

CLC number: O643 　　　　　　 **Document code:** A

Homogeneous acid catalysts such as H₂SO₄, HF, and H₃PO₄ are generally used by chemists in industrial catalytic processes [1,2]. Unfortunately, however, the inefficient separation of the catalyst from the final products and the requirement for the neutralization of the acidic waste can impose economic and environmental barriers upon the application of these acid catalysts and limit any activities focused on the broadening of their scope, leading ultimately to restrictions in their wider use in a number of other potential applications. In accordance with the principles of "green chemistry", the design of easily separable, reusable, non-toxic, low cost, and insoluble acidic catalysts has become an important area of research in chemistry [3]. In this context, the use of nanoparticles as heterogeneous catalysts has attracted considerable attention because of the interesting structural features and high levels of catalytic activity associated with these materials [4,5]. Furthermore, nanoparticle materials are considered to be a bridge between homogeneous and heterogeneous catalysts [6].

Unfortunately, however, nanoparticles are unstable and the recycling of these materials is often tedious because the recovery of these very small particles requires the use of an expensive ultra-centrifugation technique that has limited their application.

To address the issues of recyclability and reusability,

considerable efforts have been focused on the use of magnetic nanoparticles (MNPs) because their paramagnetic properties enable the trouble-free separation of the catalyst from the reaction mixture using an external magnet [7]. Unmodified MNPs tend to aggregate into large clusters because of their anisotropic dipolar attraction and this process can have a deleterious effect on the otherwise advantageous properties of the materials [8]. The aggregation associated with MNPs can be avoided by creating an electrostatic double layer [9] using a large amount of surfactants [10], or through the formation of a passive coating of inert material such as a polymer, were the presence of carbon and silica atoms on the surfaces of the iron oxide nanoparticles can assist in preventing their aggregation [11]. Furthermore, silanol moieties present on the surface can readily be functionalized via the appropriate surface modifications, enabling the introduction of a variety of different functionalities [12].

The Knoevenagel condensation is an important transformation in organic chemistry and holds a position of particular significance in organic synthesis. The reaction is predominately employed for formation of C-C double bonds during the synthesis of α,β-unsaturated carbonyl compounds. Classically, tetraketones and their enol forms have been synthesized through a combination of the Knoevenagel

condensation and Michael addition reactions of aldehydes with 1,3-cyclic diketones. These compounds are themselves key intermediates in the preparation of a variety of different heterocyclic compounds, including acridine diones [13] and xanthenes, which have been used as dyes, fluorescent materials for the visualization of bio-molecules, and in laser technologies on account of their useful spectroscopic properties [14,15]. Recently, we reported the catalyst-free synthesis of tetraketones under mild conditions in PEG-400 [16]. Unfortunately, the long reaction time required under these conditions represents a major disadvantage to this methodology. With this in mind, and given the importance and general utility of these compounds, the development of an efficient, general, and environmentally benign method for the preparation of these widely used materials is of prime importance.

1 Experimental

1.1 Preparation of catalyst

1.1.1 Preparation of nano-Fe_3O_4

The MNPs were prepared according to a previously reported procedure [17]. Typically, $FeCl_3·6H_2O$ (0.02 mol) and $FeCl_2·4H_2O$ (0.01 mol) were dissolved in distilled water (100 ml) in a three-necked round-bottom flask (250 ml). The resulting transparent solution was heated at 90 °C with rapid mechanical stirring under N_2 atmosphere for 1 h. A solution of concentrated aqueous ammonia (10 ml, 25 wt%) was then added to the solution in a drop-wise manner over a 30 min period using a dropping funnel. The reaction mixture was then cooled to room temperature and the resulting magnetic particles collected with a magnet and rinsed thoroughly with distilled water.

1.1.2 Preparation of nano-$Fe_3O_4@SiO_2$

Nano-$Fe_3O_4@SiO_2$ was synthesized according to a previously published literature method [18]. Magnetic nano particles (1.0 g) were initially diluted via the sequential addition of water (20 ml), ethanol (60 ml), and concentrated aqueous ammonia (1.5 ml, 28 wt%). The resulting dispersion was then homogenized by ultrasonic vibration in a water bath. A solution of TEOS (0.45 ml) in ethanol (10 ml) was then added to the dispersion in a drop-wise manner under continuous mechanical stirring. Following a 12 h period of stirring, the resulting product was collected by magnetic separation and washed three times with ethanol.

1.1.3 Preparation of $Fe_3O_4@SiO_2$-SO_3H

Chlorosulfonic acid (0.5 g, 4.5 mmol) was added in a drop-wise manner to a cooled (ice-bath) solution of $Fe_3O_4@SiO_2$ (1 g) in *n*-hexane (5 ml) over a 2 h period. Upon completion of the addition, the mixture was stirred for a further 3 h until to allow for the complete dissipation of HCl from the reaction vessel. The resulted MNPs were separated using an external magnet and washed with methanol before being dried in an oven at 60 °C to give $Fe_3O_4@SiO_2$-SO_3H as a brown powder. The number of H^+ sites (0.32 mmol/g) was determined by acid-base titration.

1.2 Characterization

FT-IR measurements were recorded on a Shimadzu 8400s spectrometer with KBr plates. NMR spectra were measured on a Bruker Avance-3 400 MHz instrument at 20–25 °C. Elemental analyses were performed on a Perkin-Elmer CHN analyzer 2400 series II. Melting points were determined on an Electrothermal 9100 without further corrections. Thermogravimetric analyses (TGA) were conducted on a Du Pont 2000 thermal analysis apparatus under a N_2 atmosphere at a heating rate of 10 °C/min. The sizes of MNPs were evaluated using a transmission electron microscope (TEM, 100 kV, Philips-CM 10).

To determining the acid loading of $Fe_3O_4@SiO_2$-SO_3H, a 0.1 mol/L aqueous solution of KOH (2 ml) was added to $Fe_3O_4@SiO_2$ (0.01 g) in an Erlenmeyer flask, and the resulting mixture was stirred for 15 min. The nanomagnetic catalyst was then recovered with external magnet, and the clear solution was retained for analysis. Two drops of phenolphthalein indicator were then added to the remaining solution and the resulting mixture was titrated to neutrality using a 0.1 mol/L aqueous HCl solution to determine the loading of the acid sites on the $Fe_3O_4@SiO_2$-SO_3H nanocatalyst. The H^+ loading of the nano-catalyst determined in this way was found to be 0.32 mmol/g.

1.3 Catalytic performance test

The application of $Fe_3O_4@SiO_2$-SO_3H catalyst was investigated for the synthesis of tetraketones via a combination of the Knoevenagel condensation and Michael addition reactions of aromatic aldehydes with dimedone, 1,3-indandione, or 1,3-dimethylbarbituric acid in water at room temperature (Scheme 1). In a general procedure for the synthesis of 5,5-dimethyl-2-((4,4-dimethyl-2,6-dioxocyclohexyl)(phenyl)methyl) cyclohexane-1,3-dione, a mixture of dimedone (0.28 g, 2 mmol), benzaldehyde (0.21 g, 1 mmol), and $Fe_3O_4@SiO_2$-SO_3H (0.01 g) in H_2O (6 ml) was stirred for 80 min at room temperature. Upon completion of the reaction (monitored by TLC), the catalyst was separated from the solid crude product using an external magnet. The
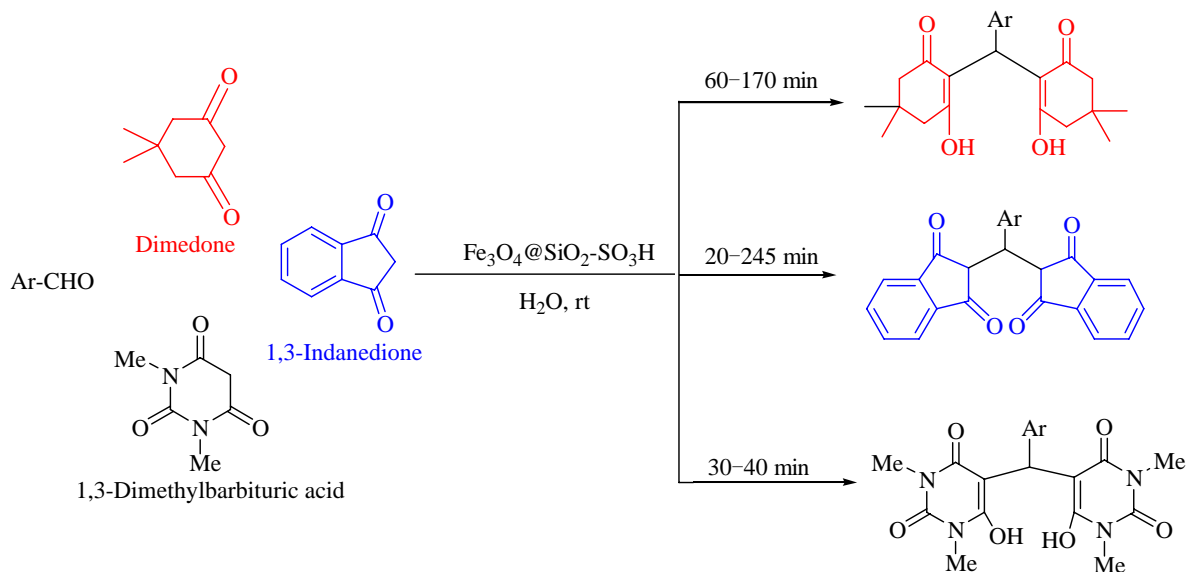
Scheme 1. Synthesis of the tetraketones catalyzed by $Fe_3O_4@SiO_2\text{-}SO_3H$.

precipitated solid was then filtered and the filter-cake collected and crystallized from ethanol to afford the pure product. Yield 97%, 0.35 g, m.p. 194–195 °C.

All of the products generated in this way were characterized by comparison of their spectral (IR, ^1H NMR), TLC, and melting point data with those of the authentic samples. Upon completion of the catalytic reactions, the catalyst was separated from the solid crude product using an external magnet. The precipitated solid was then filtered and the filter-cake collected and dissolved in hot EtOH, and any remaining catalyst was removed magnetically. The recovered catalyst was subsequently washed with acetone and MeOH and dried at 60 °C to give recycled $Fe_3O_4@SiO_2\text{-}SO_3H$. The spectral (IR, ^1H NMR, ^{13}C NMR) and analytical data for new compounds are as follows.

3-Hydroxy-2-((2-hydroxy-4,4-dimethyl-6-oxocyclohex-1-enyl)(3,4-dimethoxyphenyl)methyl)-5,5-dimethylcyclohex-2-enone. m.p. 183–185 °C. ^1H NMR (400 MHz, CDCl₃): δ 1.14 (s, 6H), 1.26 (s, 3H), 1.29 (s, 3H), 2.50–2.33 (m, 8H), 3.79 (s, 3H), 3.85 (s, 3H), 5.53 (s, 1H), 6.66 (d, $J = 8.4$ Hz, 2H), 6.81 (d, $J = 8.0$ Hz, 1H), 11.68 (s, br, 1H), 12.01 (s, br, 1H); ^{13}C NMR (100 MHz, CDCl₃): δ 28.5, 29.65, 30.28, 50.35, 51.59, 55.21, 56.13, 108.81, 111.32, 114.15, 115.21, 122.40, 135.52, 146.81, 149.87, 180.98, 181.00, 198.94, 199.57; IR (KBr, cm⁻¹): v 2962, 2839, 1589. Anal. calcd for C₂₅H₃₂O₆: C 70.09, H 7.47; found: C 70.01, H 7.52.

3-Hydroxy-2-((2-hydroxy-4,4-dimethyl-6-oxocyclohex-1-enyl)(naphthalen-2-yl)methyl)-5,5-dimethylcyclohex-2-enone. m.p. 204–206 °C. ^1H NMR (400 MHz, CDCl₃): δ 1.16 (s, 6H), 1.34 (s, 6H), 2.35–2.56 (m, 8H), 5.722 (s, 1H), 7.25–7.26 (m, 1H), 7.45–7.55 (m, 3H), 7.72–7.79 (m, 3H), 11.63 (s, br, 0.67H), 11.98 (s, 1H); ^{13}C NMR (100 MHz, CDCl₃): δ 27.45, 29.72, 31.52, 33.04, 46.49, 47.11, 115.63,

125.39, 125.45, 125.94, 127.48, 127.84, 127.89, 131.84, 133.29, 135.59, 189.56, 190.58; IR (KBr, cm⁻¹): v 28.77, 2630, 1589. Anal. calcd for C₂₇H₃₀O₄: C 77.51, H 7.17; found: C 77.45, H 7.08.

2-(4-(Dimethylamino)benzylidene)-2H-indene-1,3-dione. m.p. 207–209 °C. ^1H NMR (400 MHz, CDCl₃): δ 3.18 (s, 6H), 6.78 (d, $J = 9.2$ Hz, 2H), .74–7.76 (m, 2H), 7.82 (s, 1H), 7.95 (s, br, 1H), 8.57 (d, $J = 8.4$ Hz, 2H); ^{13}C NMR (100 MHz, CDCl₃): δ 40.24, 45.76, 110.61, 120.39, 122.08, 123.17, 123.18, 128.26, 133.96, 135.01, 135.19, 135.41, 140.05, 141.35, 148.35, 150.52, 189.27, 190.58; IR (KBr, cm⁻¹): v 1658, 1512. Anal. calcd for C₁₈H₁₅NO₂: C 77.97, H 5.41, N 5.05; found: C 77.91, H 5.30, N 4.98.

5-((1,2,3,4-Tetrahydro-6-hydroxy-1,3-dimethyl-2,4-dioxopyrimidin-5-yl)(4-nitrophenyl)methyl)-6-hydroxy-1,3-dimethylpyrimidine-2,4(1H,3H)-dione. m.p. 165–169 °C. ^1H NMR (400 MHz, CDCl₃): δ 3.21–3.67 (m, 12H), 5.69 (s, 1H), 7.39 (d, $J = 7.6$ Hz, 1H), 7.77 (d, $J = 7.2$ Hz, 1H), 8.19–8.29 (m, 2H), 13.53 (s, br, 0.46H); ^{13}C NMR (100 MHz, CDCl₃): δ 28.90, 29.08, 29.15, 29.47, 34.90, 50.56, 68.13, 92.77, 123.21, 127.52, 129.19, 130.21, 146.65, 150.32, 163.31, 164.73; IR (KBr, cm⁻¹): v 2951, 1697, 1627. Anal. calcd for C₁₉H₁₉N₅O₈: C 51.23, H 4.26, N 15.73; found: C 51.17, H 4.33, N 15.64.

5-((4-Bromophenyl)(1,2,3,4-tetrahydro-6-hydroxy-1,3-dimethyl-2,4-dioxopyrimidin-5-yl)methyl)-6-hydroxy-1,3-dimethylpyrimidine-2,4(1H,3H)-dione. m.p. 182–185 °C. ^1H NMR (400 MHz, CDCl₃): δ 3.19–3.57 (m, 12H), 5.54 (s, 1H), 7.39 (d, $J = 7.6$ Hz, 1H), 7.41 (d, $J = 7.2$ Hz, 1H), 7.59–7.64 (m, 2H), 12.21 (s, br, 0.66H); ^{13}C NMR (100 MHz, CDCl₃): δ 28.90, 29.08, 29.15, 29.47, 34.78, 74.13, 120.29, 127.52, 129.17, 131.22, 141.21, 142.65, 150.32, 151.54,   163.31, 164.73 184,11, 186.35; IR (KBr, cm⁻¹): v

2954, 1666, 1542. Anal. calcd for $C_{19}H_{19}BrN_4O_6$: C 47.60, H 3.96, N 11.69; found: C 47.51, H 4.10, N 11.58.

5-(4-Methoxybenzylidene)-1,3-dimethylpyrimidine-2,4,6 (1H,3H,5H)-trione. m.p. 174–177 °C. ^{1}H NMR (400 MHz, CDCl$_3$): δ 3.37 (s, 3H), 3.44 (s, 3H), 3.92 (s, 3H), 6.96 (d, J = 8.4 Hz, 1H), 7.04 (t, J = 7.6 Hz, 1H), 7.50–7.54 (m, 1H), 8.06 (d, J = 8 Hz, 1H), 8.92 (s, 1H); ^{13}C NMR (100 MHz, CDCl$_3$): δ 28.38, 28.97, 55.77, 110.46, 117.33, 119.76, 122.13, 132.70, 134.61, 155.31, 159.60, 160.44, 162.60; IR (KBr, cm^{-1}): ν 1666, 1581. Anal. calcd for $C_{14}H_{14}N_2O_4$: C 61.31, H 5.10, N 10.21; found: C 61.25, H 5.17, N 10.13.

2 Results and discussion

In our continuing efforts towards the development of efficient and environmentally benign synthetic methodologies [19–24], herein, we report the simple preparation of nano-Fe$_3$O$_4$ encapsulated-silica nanoparticles bearing sulfonic acid groups as a magnetically recoverable catalyst. The MNPs were prepared via a chemical co-precipitation [25] and were subsequently coated with a layer of silica using the sol-gel method [26] to provide reaction sites for further functionalization and thermal stability. The Fe$_3$O$_4$@SiO$_2$ nanoparticles were then transformed to Fe$_3$O$_4$@SiO$_2$-SO$_3$H via a condensation reaction with chlorosulfonic acid in *n*-hexane to afford a dark brown powder with a H$^+$ loading of 0.32 mmol/g, as determined by simple titration. The resulting MNP acid catalyst was characterized by FT-IR, particle induced X-ray emission (PIXE), TEM, and TGA.

FT-IR analysis was used to characterize the presence of the –SO$_3$H groups on the surface of the MNPs (Fig. 1). As shown in Fig. 1(3), the FT-IR spectrum of Fe$_3$O$_4$@SiO$_2$-SO$_3$H was clearly different from those of Fe$_3$O$_4$ (Fig. 1(1)) and Fe$_3$O$_4$@SiO$_2$ (Fig. 1(2)). The broad band at around 3500–3000 cm^{-1} was attributed to adsorbed
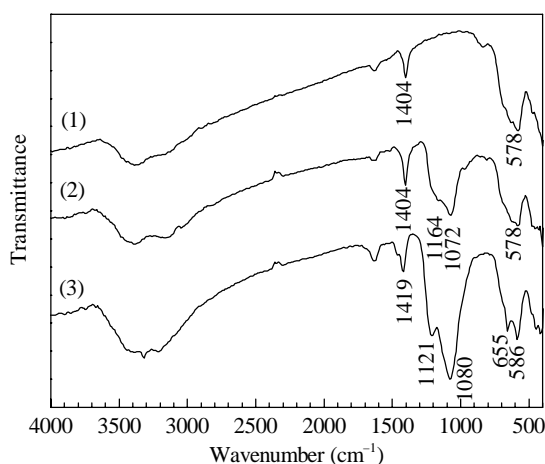

Fig. 1. FT-IR spectra of Fe$_3$O$_4$ (1), Fe$_3$O$_4$@SiO$_2$ (2), and Fe$_3$O$_4$@SiO$_2$-SO$_3$H (3).

water. The strong absorption at 578 cm^{-1} was characteristic of the Fe–O stretching vibration (Fig. 1(1) and 1(2)). For Fe$_3$O$_4$@SiO$_2$-SO$_3$H, the Fe–O vibration bands were shifted to 586 cm^{-1} because of quantum confinement (Fig. 1(3)). Bands corresponding to Si–O–Si stretching appeared at 1072 cm^{-1}, whereas the absorption band at 1419 cm^{-1} (corresponding to asymmetric SO$_2$ stretching) and the broad peak in range of 1080–1211 cm^{-1} (attributed to the overlapping of peaks corresponding to Si–O–Si, Fe–O–Si, and symmetric SO$_2$ stretching) indicated that the MNPs possessed SO$_3$H groups.

The PIXE spectrum of Fe$_3$O$_4$@SiO$_2$-SO$_3$H indicated the presence of Fe, Si, and S (Fig. 2). The PIXE results were in good agreement with the FT-IR analysis (Table 1).
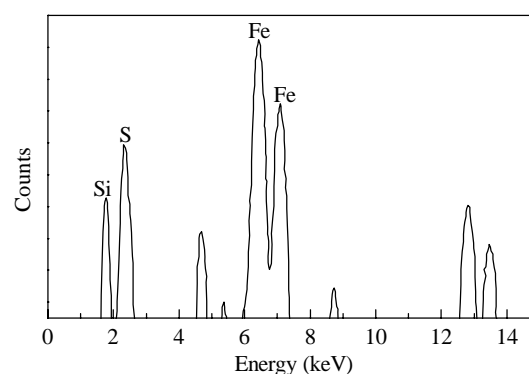

Fig. 2. PIXE spectrum of Fe$_3$O$_4$@SiO$_2$-SO$_3$H.

Table 1 Concentrations of the elements in Fe$_3$O$_4$@SiO$_2$-SO$_3$H as their oxide forms determined by PIXE and titration

Element	Concentration by PIXE (10^{-6})	Concentration by titration (%)
Si	21587	—
S	69799	10.00
Fe	606011	—

TGA was used to study the thermal stability of the acid catalyst (Fig. 3). The TGA curve was divided into several regions corresponding to different mass lose ranges. The first region, which occurred below 150 °C, displayed a mass loss that was attributable to the loss of adsorbed solvent or trapped water from the catalyst. A mass loss of approximately 10% weight occurred between 150 and 500 °C that was likely a consequence of the loss of SO$_3$H groups. The occurrence of further mass losses at higher temperature resulted from the decomposition of silica shell [27]. Thus, the catalyst was stable up to 250 °C, confirming that it could be safely used in organic reactions at temperatures in the range of 80–140 °C.

TEM analysis revealed that the Fe$_3$O$_4$@SiO$_2$-SO$_3$H nanoparticles were uniform in size with an average diameter around 15 nm (Fig. 4).
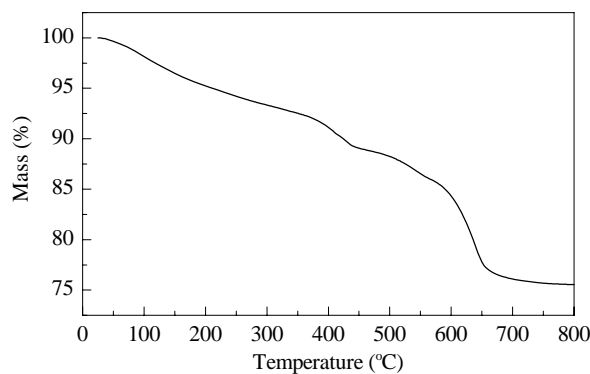
Fig. 3.   TGA curve of Fe$_3$O$_4$@SiO$_2$-SO$_3$H.
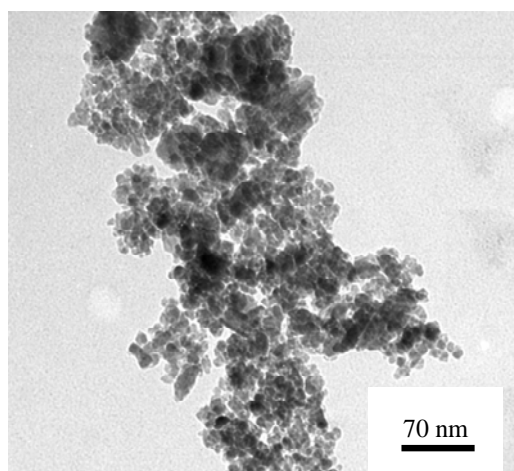

70 nm

Fig. 4.   TEM image of Fe$_3$O$_4$@SiO$_2$-SO$_3$H.

Having synthesized and fully characterized the Fe$_3$O$_4$@SiO$_2$-SO$_3$H, its role as a catalyst was evaluated for the synthesis of tetraketones. We initially investigated a model reaction between dimedone and benzaldehyde in H$_2$O. From the results provided in Table 2, it was clear that Fe$_3$O$_4$@SiO$_2$-SO$_3$H performed well to give the desired product within 80 min in 98% yield at room temperature. For comparison, the model reaction was performed using nano-Fe$_3$O$_4$ and Fe$_3$O$_4$@SiO$_2$, which gave the desired product in 63% and 54% yield, respectively (Table 2, entries 2 and 3). These results confirmed that Fe$_3$O$_4$@SiO$_2$-SO$_3$H performed more effectively as a catalyst than the original homogeneous catalyst. The greater catalytic activity of Fe$_3$O$_4$@SiO$_2$-SO$_3$H was most likely related to the SO$_3$H groups of the catalyst, which could provide efficient acidic sites. Furthermore, this catalyst performed more efficiently than silica sulfuric acid (SSA) with respect to the yield and time of the model reaction under the same conditions, with the difference here being attributed to the larger surface area offered by the nanoscale heterogeneous catalyst (Table 2, entry 5).

The model reaction was also investigated in several other

Table 2   Optimization of the reaction conditions for the synthesis of tetraketones

Entry	Catalyst	Catalyst loading (mg)	Solvent	Time (min)	Yield (%)
1	—	—	H$_2$O	80	trace
2	Nano-Fe$_3$O$_4$	10	H$_2$O	80	63
3	Fe$_3$O$_4$@SiO$_2$	10	H$_2$O	80	54
4	Fe$_3$O$_4$@SiO$_2$-SO$_3$H	10	H$_2$O	80	98
5	SSA	10	H$_2$O	80	77
6	Fe$_3$O$_4$@SiO$_2$-SO$_3$H	15	H$_2$O	80	98
7	Fe$_3$O$_4$@SiO$_2$-SO$_3$H	5	H$_2$O	80	76
8	Fe$_3$O$_4$@SiO$_2$-SO$_3$H	10	EtOH	120	76
9	Fe$_3$O$_4$@SiO$_2$-SO$_3$H	10	CH$_3$CN	120	54
10	Fe$_3$O$_4$@SiO$_2$-SO$_3$H	10	CH$_2$Cl$_2$	120	trace
11	Fe$_3$O$_4$@SiO$_2$-SO$_3$H	10	EtOAc	120	trace

Reaction conditions: dimedone 2 mmol, benzaldehyde 1 mmol, solvent 6 ml, room temperature.

solvent to further investigate the efficiency of the catalyst (Table 2, entries 4 and 8–11). Based on reaction yield alone, the best transformation was observed when the reaction was performed in H$_2$O, indicating that the solvent polarity could play an important role in the process. The reaction was also investigated with different catalyst loading, revealing that 10 mg (10 mol%) of catalyst provided the best results in terms of reaction time, economy of catalyst charge, and reaction yield (Table 2, entries 4, 6, and 7). In a control experiment, the reaction was performed without the catalyst and only a trace amount of the product was observed, confirming that the Fe$_3$O$_4$@SiO$_2$-SO$_3$H material was performing as a catalyst in the transformation.

To evaluate the scope and limitations of this methodology, we extended our studies to include a variety of structurally different arylaldehydes and initially examined the reaction of dimedone with several different aldehydes. The results are summarized in Table 3 (Table 3, entries 1–18). In almost all cases, the reactions proceeded smoothly within 65–170 min, providing the corresponding products in excellent isolated yields. It is noteworthy that the use of bulky aldehydes such as naphthalene 2-carbaldehyde, afforded the corresponding product in high yield without the formation of any side products (Table 3, entry 15). In contrast, the use of an aliphatic aldehyde gave the corresponding compound in a lower yield (Table 3, entry 18).

Encouraged by these results, we also attempted to prepare tetraketone derivatives from other 1,3-cyclic diketones to further broaden the scope of our novel catalytic transformation. Pleasingly, the reaction of a variety of different arylaldehydes with 2 equivalents of 1,3-indanedione (Table 3, entries 19–25) or 1,3-dimethylbarbituric acid (Table 3, entries 26–28) resulted in the formation of the corresponding desired products in high yields. Interestingly, benzaldehydes

Table 3 Synthesis of tetraketones catalyzed by Fe₃O₄@SiO₂-SO₃H

| Entry | Ar-CHO | Diketone | Time (min) | Yield[a] (%) | Melting point (°C) | |
					Found	Reported
1	C₆H₅	dimedone	80	97	194–195	194–195 [16]
2	4-Br-C₆H₄	dimedone	88	75	172–173	172–174 [28]
3	3-Br-C₆H₄	dimedone	66	97	196–198	184–186 [27]
4	4-MeO-C₆H₄	dimedone	90	95	185–187	185–186 [27]
5	2-MeO-C₆H₄	dimedone	65	93	185–186	181–183 [27]
6	4-NO₂-C₆H₄	dimedone	60	97	189–191	188–190 [29]
7	3-NO₂-C₆H₄	dimedone	130	95	197–199	196–198 [27]
8	4-Me-C₆H₄	dimedone	115	81	141–142	141–142 [30]
9	4-Cl-C₆H₄	dimedone	80	83	144–146	145–146 [29]
10	2-Cl-C₆H₄	dimedone	95	93	203–205	203–205 [30]
11	2,4-Cl₂-C₆H₃	dimedone	100	90	202–204	203–204 [30]
12	2-OH-C₆H₄	dimedone	85	97	208–209	205–206 [30]
13	3,4-(MeO)₂C₆H₄	dimedone	170	91	183–185	—
14	4-(Me₂N)-C₆H₄	dimedone	110	63	195–197	194–195 [27]
15	Naphthalene 2-carbaldehyde	dimedone	90	95	204–206	—
16	4-F-C₆H₄	dimedone	85	75	184–186	185–187 [16]
17	2-Thiophen	dimedone	65	78	155–158	156–158 [16]
18	C₆H₅CH=CH	dimedone	100	44	215–217	215–126 [30]
19	4-NO₂-C₆H₄	1,3-indanedione	20	97	198–199	197–199 [16]
20	3-Br-C₆H₄	1,3-indanedione	220	95	168–170	169–170 [16]
21	4-Me-C₆H₄	1,3-indanedione	245	88	171–173	172–174 [16]
22	2-Cl-C₆H₄	1,3-indanedione	210	81	166–168	165–167 [16]
23	4-(Me₂N)-C₆H₄	1,3-indanedione	125	87	207–209[b]	—
24	C₆H₅	1,3-indanedione	85	89	163–164	162 [27]
25	4-Cl-C₆H₄	1,3-indanedione	185	92	154–156	153–155 [16]
26	4-NO₂-C₆H₄	1,3-dimethylbarbituric acid	30	91	165–169	—
27	4-Br-C₆H₄	1,3-dimethylbarbituric acid	40	87	182–185	—
28	4-MeO-C₆H₄	1,3-dimethylbarbituric acid	35	95	174–177[b]	—

Reaction conditions: arylaldehyde 1 mmol, diketone 2 mmol, H₂O 6 ml, catalyst 10 mg, room temperature.
[a]Isolated yield. [b]The Knoevenagel condensation products.

bearing strong electron donating groups only produced the Knoevenagel condensation products with 1,3-indanedione [16] and 1,3-dimethylbarbituric acid (Table 3, entries 23 and 28, Scheme 2).
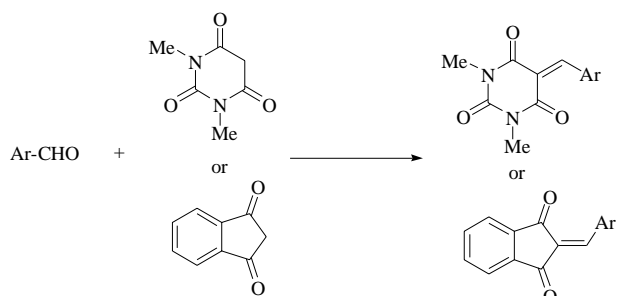
Scheme 2. Knoevenagel condensation catalyzed by Fe₃O₄@SiO₂-SO₃H.

From a green chemistry perspective, experiments concerning the recycling and reuse of the catalyst were carried out. Upon completion of the reaction, the catalyst was simply recovered with an external magnet, washed with methanol, and dried at 60 °C for 1 h. The recovered catalyst was then added to a fresh reaction mixture under the same conditions. The catalyst could be efficiently recovered and recycled up to three times without suffering any significant drop in its catalytic activity or the yield for the reaction (Table 4). Unfortunately, however, further recycling of the nanocatalyst led to significant losses in its activity, with these losses being linked to the gradual loss of the catalyst during the filtration and washing stages.

Table 4 Recycling of the Fe₃O₄@SiO₂-SO₃H catalyst

Number of cycle	Yield (%)
1	97
2	95
3	90
4	73
5	49

Reaction conditions: benzaldehyde 1 mmol, dimedone 2 mmol, catalyst 10 mg, H₂O 6 ml, room temperature.

3 Conclusions

Fe$_3$O$_4$@SiO$_2$-SO$_3$H MNPs can be used for the synthesis of tetraketones via the sequential Knoevenagel condensation and Michael addition reactions of aromatic aldehydes with 1,3-cyclic diketones. This active catalyst is thermally stable, green, inexpensive, and easy to prepare. In addition, it could be easily separated from the reaction mixture and recycled up to three times without any significant impact on its activity or the reaction yields. The operational simplicity, high yields, and facile work-up procedures associated with this catalytic process represent some of the other advantages of this methodology.

References

1 Cole-Hamilton D J. *Science*, 2003, **299**: 1702

2 Baker R T, Tumas W. *Science*, 1999, **284**: 1477

3 Nasir Baig R B, Varma R S. *Green Chem*, 2012, **14**: 625

4 Schatz A, Reiser O, Stark W J. *Chem Eur J*, 2010, **16**: 8950

5 Yan N, Xiao C X, Kou Y. *Coord Chem Rev*, 2010, **254**: 1179

6 Deng J, Mo L-P, Zhao F-Y, Hou L-L, Yang L, Zhang Z-H. *Green Chem*, 2011, **13**: 2576

7 Koukabi N, Kolvari E, Khazaei A, Zolfigol M A, Shirmardi-Shaghasemi B, Khavas H R. *Chem Commun*, 2011, **47**: 9230

8 Li Z W, Zhu Y F. *Appl Surf Sci*, 2003, **211**: 315

9 Younes H, Christensen G, Luan X N, Hong H D, Smith P. *J Appl Phys*, 2012, **111**: 064308

10 Shao H, Lin T, Luo J, Guo Z. *Adv Mater Res*, 2011, **335-336**: 951

11 Benelmekki M, Xuriguera E, Caparros C, Rodríguez-Carmona E, Mendoza R, Corchero J L, Lanceros-Mendez S, Martinez L. *J Colloid Interf Sci*, 2012, **365**: 156

12 Liu Y-H, Deng J, Gao J-W, Zhang Z-H. *Adv Synth Catal*, 2012, **354**: 441

13 To Q H, Lee Y R, Kim S H. *Bull Korean Chem Soc*, 2012, **33**: 1170

14 Kumaran R, Varalakshmi T, Malar E J, Padma R P. *J Fluoresc*, 2010, **20**: 993

15 Odo J, Torimoto S-I, Nakanishi S, Niitani T, Aoki H, Inoguchi M, Yamasaki Y. *Chem Pharm Bull*, 2012, **60**: 846

16 Nemati F, Kiani H. *Chin J Chem*, 2011, **29**: 2407

17 Rafiee E, Eavani S. *Green Chem*, 2011, **13**: 2116

18 Yang D, Hu J, Fu S. *J Phys Chem C*, 2009, **113**: 7646

19 Nemati F, Kiani H. *Chin Chem Lett*, 2010, **21**: 403

20 Nemati F, Kiani H, Hayeniaz Y S. *Synth Commun*, 2011, **41**: 2985

21 Nemati F, Fakhai A S, Amoozadeh A, Hayeniaz Y S. *Synth Commun*, 2011, **41**: 3695

22 Nemati F, Arghan M, Amoozadeh A. *Synth Commun*, 2012, **42**: 33

23 Nemati F, Bigdeli M A, Mahdavinia G H, Kiani H. *Green Chem Lett*, 2010, **3**: 89

24 Bigdeli M A, Nemati F, Mahdavinia G H. *Tetahedron Lett*, 2007, **48**: 6801

25 Bee A, Massart R, Neveu S. *J Magn Magn Mater*, 1995, **149**: 6

26 Ferreira R V, Pereira I L S, Cavalcante L C D, Gamarra L F, Carneiro S M, Amaro E Jr, Fabris J D, Domingues R Z, Andrade A L. *Hyperfine Interact*, 2010, **195**: 265

27 Yu J-J, Wang L-M, Liu J-Q, Guo F-L, Liu Y, Jiao N. *Green Chem*, 2010, **12**: 216

28 Zhang Y, Shang Z C. *Chin J Chem*, 2010, **28**: 1184

29 Kaupp G, Naimi-Jamal M R, Schmeyers J. *Tetrahedron*, 2003, **59**: 3753

30 Jin T S, Zhang J S, Wang A-Q, Li T-S. *Synth Commun*, 2005, **35**: 2339